PERGAMON

International Journal of Solids and Structures 36 (1999) 557–574

INTERNATIONAL JOURNAL OF SOLIDS and STRUCTURES

On the axial propagation of kink bands in fiber composites: Part I experiments

T. J. Vogler, S. Kyriakides*

Research Center for Mechanics of Solids, Structures and Materials The University of Texas at Austin, WRW 110, Austin, TX 78712, U.S.A.

Received 13 August 1997; in revised form 12 January 1998

Abstract

In many fiber composites, longitudinal compressive failure leads to the formation of kink bands. It has been found that these kink bands, once formed, can be made to propagate (broaden) in a steady-state manner at a constant stress level called the propagation stress (σ_P). This is a characteristic stress of the material which, for the AS4/PEEK composite used in the study reported here, is approximately 40% of its compressive strength. This phenomenon is investigated experimentally using a special confining set-up that allows direct observation of the propagation process. For the composite studied, the kink bands have a repeatable inclination (β) of approximately 15°, and the fibers within the bands are rotated to about 30° in the absence of a load. When loaded to σ_P, however, they are found to rotate further to 40°, that is, substantially greater than the 2β reported elsewhere. The mechanism of propagation is found to be a bend-break-rotate sequence undergone by short segments of fibers at the edge of the kink band. It is well known that polymeric matrix composites such as the one used in this study exhibit rate-dependent behavior. Experimental results are presented which show that the kink band propagation stress is also rate dependent.

1. Introduction

It has recently been discovered that, under compression, composites can exhibit significant post-failure strength and 'ductility' (Moran and Shih, 1997; Vogler and Kyriakides, 1997). The initial failure is associated with fiber microbuckling which localizes and results in bands of kinked fibers. The bands have distinct orientations, but their width depends on the energy available from the unloading of surrounding material during the incipient load drop. In displacement controlled experiments on approximately square plates (48×48 mm) presented in V and K (1997), the initial failure led to the formation of a single kink band with an inclination of approximately 15° and a

* Author to whom correspondence should be addressed. E-mail: skk@mail.utexas.edu

0020–7683/99/$ - see front matter
PII: S0020–7683(98)00029–8

width of the order of 250 fiber diameters ($h = 7\mu m$). Following this initial transient event, the load stabilized at a level corresponding to approximately 35–40% of the compressive strength of the composite. Under continued compression, the band inclination remained constant, but the band width grew in a steady-state manner at a constant stress level. This is referred to as *axial propagation* or *broadening* of the kink band, and the stress required for quasi-static propagation is defined as the *propagation stress* (σ_P) of the composite. (Evidence of band broadening under more complex conditions was also reported in Moran et al. (1995) and Kyriakides and Ruff (1997). It was found that the band broadened by progressive addition of narrow zones of fibers from the adjoining intact material which bend into the inclined band and eventually break and align themselves with the rotated kinked material. The photograph in Fig. 1a shows one of the test specimens in which the band was propagated to a width (w) of approximately 400 h (the geometric variables of the problem are defined in Fig. 1b). Provided the two intact portions of the plate above and below the kink band were allowed to displace freely (in the x_2-direction) relative to each other, the axial propagation of the kink band could be continued, providing a hitherto unknown mechanism of ductility and energy absorption for composites.

A different phenomenon involving steady-state propagation of out-of-plane kinking across a thin composite plate was reported by Sivashanker et al. (1995). This propagation phenomenon is one characteristic of thin laminates rather than of bulk composite as is the case here, and the propagation stresses measured were of the order of 30% of the values of σ_P reported in V and K (1997) (albeit for a different material system). Further, their σ_P depends strongly on the thickness of the laminate and the test conditions used (V and K, 1997).

Steady-state axial propagation of kink bands in an IM7/PEEK composite was also observed independently by Moran and Shih (1998) who also tried to model the phenomenon. The fiber rotation inside the kink band (ϕ in our notation) was assumed to be equal to twice the band inclination (β). Furthermore, the composite shear response was assumed to exhibit a recovery of hardening at large strains ($\gamma > 0.3$). An elegant model of steady-state band broadening has recently been proposed by Budiansky et al. (1997). Here the fibers bend but do not break, while their maximum rotation is also limited to be 2β. [Non-breaking kinked fibers have been reported by Moran and Shih (1998) for IM7/PEEK and by Fleck et al. (1997) for IM8/PEEK]. The assumption that kinked material shears to $\phi = 2\beta$ stems from the fact that at this angle the deformation is volume preserving. To the best of our knowledge, this was first suggested by Paterson and Weiss (1966) from observations of kink bands in phyllite—they also cite an even earlier (1898) observation by Mügge. The idea seems to have been transferred to composites by Weaver and Williams (1975) and was later adopted by Chaplin (1977). Numerous authors since have accepted and used this premise e.g. Evans and Adler (1978); Fleck and Budiansky (1991); Moran et al. (1995); Sivashanker et al. (1995); Moran and Shih (1997). A notable exception is Steif (1990) who predicted rotation angles larger than 2β via a simple model. A fact that has gone unnoticed is that in all cases where the rotation angles were actually measured the specimens were in an unloaded state.

In our previous work on this subject (V and K, 1997), we reported that, although in the absence of load our kinked composite was found to shear to approximately 2β, the deformation was observed to increase as the specimen was loaded so that at the propagation stress it was significantly larger than 2β. This conclusion was reached from estimates of the angle ϕ made from local measurements of the overall axial (δ) and transverse (v) displacements of the plate specimens traversed by a kink band (Fig. 1b). Because of the importance of this issue to the modeling of the

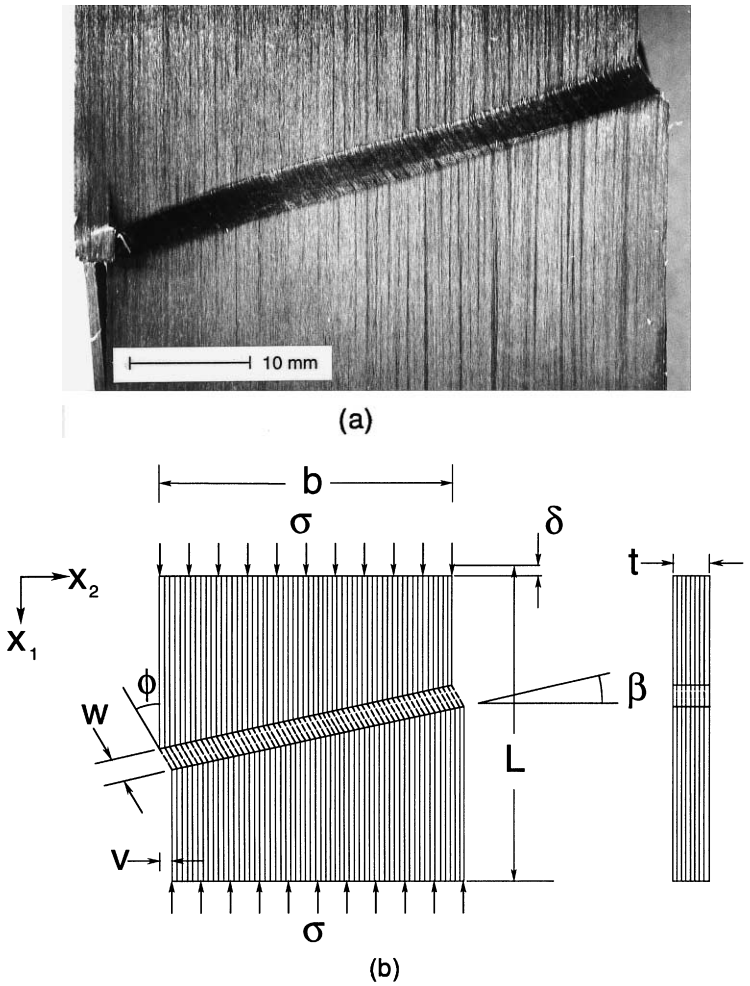

Fig. 1. A kink band in a composite plate: (a) photograph and (b) drawing with definitions of geometric parameters.

phenomenon, the subject is revisited. In this paper, we present results from new experiments in which the deformation inside the kink band is measured directly. In addition, new experimental results showing that the propagation stress of our AS4/PEEK composite exhibits significant rate sensitivity are also presented. A model of steady-state axial propagation of kink bands follows in the accompanying paper along with a critical review of its performance vis-á-vis that of other models.

2. Experimental set-up

The experiments involved axial compression of composite plates tested under approximately plane strain conditions. The experiment set-up was similar to the one described in V and K (1997) but was modified to enable direct measurement of the kinked fiber rotation. The material tested was again an AS4/PEEK unidirectional composite with a fiber volume fraction of $\upsilon_f = 0.60$. Its elastic mechanical properties are given in Table 1. The plates were 0.300 in (7.6 mm) thick, 1.86 in (47.2 mm) tall and 1.6–2.0 in (41–51 mm) wide. The specimens were ground to ensure smooth and parallel surfaces, and the corners were rounded to reduce stress concentrations. The top and bottom of the specimen were potted into steel end caps with 0.13 in (3.3 mm) deep slots with an epoxy adhesive for better load transfer. Two well-lubricated 1/2 inch (13 mm) thick hardened steel plates with ground surfaces were clamped onto the lateral surfaces. This clamping was shown previously to restrict the deformation inside the kink band to be essentially planar.

The assembly, shown schematically in Fig. 2, was placed between parallel platens mounted on a universal testing machine. A linear roller bearing between the test assembly and the lower platen allowed the upper and lower parts of the specimen to displace horizontally (x_2-direction) relative to each other during the formation and subsequent propagation of a kink band. A miniature displacement transducer (LVDT) was mounted across the end caps for a more direct monitoring of the shortening of the specimen. A second LVDT was used to measure the horizontal displacement of the end caps relative to each other. The signals from these transducers, as well as those corresponding to the load and testing machine displacement, were monitored and recorded using a computer operated data acquisition system.

Specimens were compressed at relatively slow, constant, end-displacement rates ($\dot{\delta} \sim 10^{-4}$–$10^{-1}$

Table 1
Mechanical properties of the composite tested

AS4/PEEK Composite				
E_{11} msi (GPa)	E_{22} msi (GPa)	G_{12} msi (GPa)	ν_{12}	υ_f
18.62 (128)	1.533 (10.57)	0.84 (5.79)	0.3	0.60

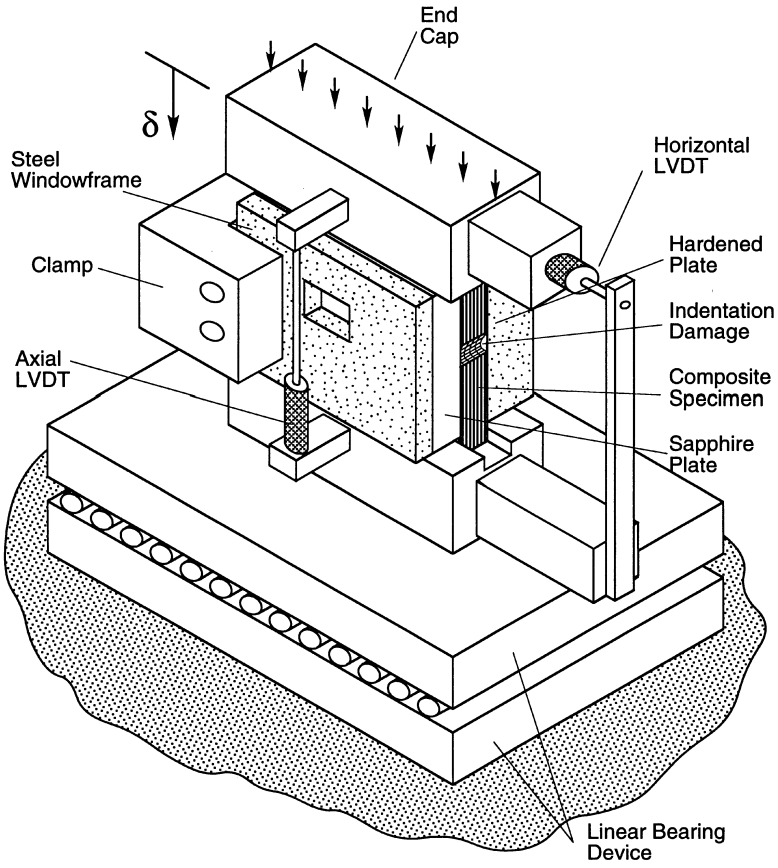

Fig. 2. Schematic of test fixture for uniaxial compression of composite plates.

in/min). The onset of failure was facilitated by indenting one side of the specimen at mid-height with a 0.093 in (2.4 mm) diameter, hardened steel rod as described in V and K (1997). This reduced the stress required to initiate failure (σ_1) to a level corresponding to approximately 60% of the failure stress of the intact composite. Despite this reduction, initiation of the kink band occurred dynamically and, as before, resulted in full plate width bands, approximately 250 h wide. When direct observation of the kink band during further loading was desired, the experiment was interrupted at this stage, the load was removed and one of the steel side plates was replaced by a synthetic sapphire (Al_2O_3) plate. The sapphire plate was transparent and had optically smooth surfaces. It was 0.50 in (13 mm) thick, and covered the whole specimen. A ground finished protective steel plate with a cut-out window (0.52×0.46 in–13×12 mm) was placed over the sapphire and the assembly was clamped back together as shown in Fig. 2.

During subsequent loading, the kink band was monitored through the window by a microscope. In some of the experiments, a microscope coupled with an Optronics CS450 CCD camera (768×493 pixels) was used to obtain a continuous, real-time video recording of the events. In other experiments, a high-resolution digital camera (Kodak Megaplus model 4.2 with 2029×2044 pixel resolution) with a microscope lens was used in conjunction with the NIH Image Analysis program

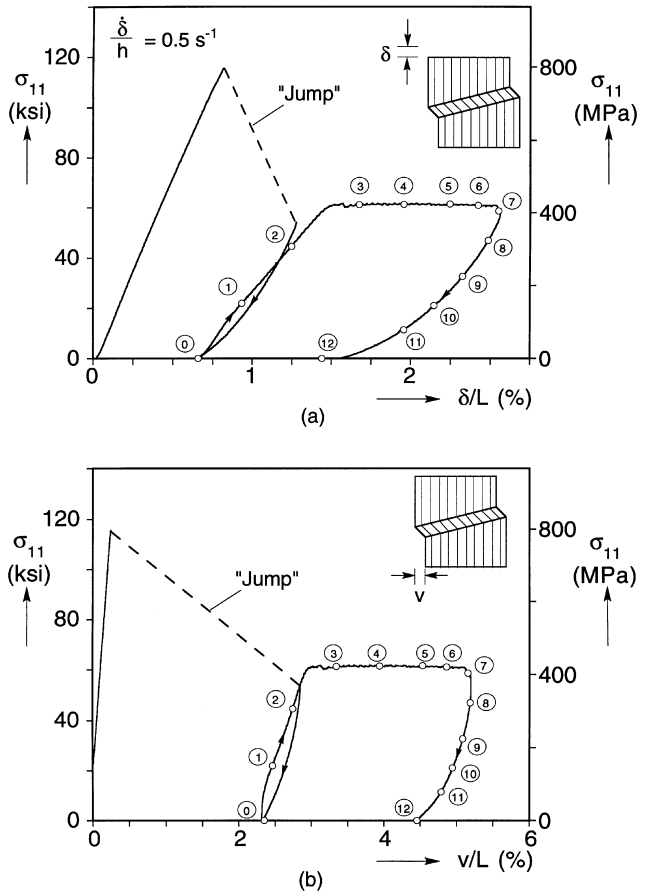

Fig. 3. (a) Typical axial stress-end shortening response (b) and axial stress-horizontal displacement response for a composite specimen showing kink band initiation and steady-state propagation.

to record discrete views of the events. Such digital images could subsequently be enhanced using the Adobe Photoshop software.

3. Results

3.1. Kink band propagation

We now present the results of a typical experiment of this type. The dimensions of the composite plate were: $b = 1.703$ in (43.26 mm), $L = 1.859$ in (47.22 mm) and $t = 0.297$ in (7.54 mm). The specimen was compressed at a displacement rate of 0.008 in/min (0.2 mm/min) which, during the initial homogeneous deformation, resulted in a strain rate of 7×10^{-5} s^{-1}. The axial stress-end shortening response recorded is shown in Fig. 3a. Initially, the response was nearly linear with a slope of 15.0 msi (103 GPa). This slope is somewhat lower than the elastic modulus of the material

because some deformation of the steel end-caps is included in the local value of δ measured. Failure initiates at the point of indentation at a stress level of 115.6 ksi (797.2 MPa). This compares with the strength of the undamaged material of 175 ksi ($\sim$1.2 GPa) (Kyriakides et al. 1995). Failure involves the dynamic formation of a kink band which traverses the specimen. It is accompanied by a drop in load to 53.7 ksi (370 MPa) and a sudden shortening in the measured end of 0.0084 in (0.2134 mm). Although the 225 kip (1 MN) testing machine used is quite stiff, in the configuration of this test the effective 'spring constant' of the machine and the other accessories involved is smaller than that of the specimen. Thus, the load drop associated with the initiation of the kink band results in an energy release from the machine which feeds into the kink band. The jump in the local value of δ is a consequence of this unloading.

The recorded relative axial stress is plotted in Fig. 3b as a function of the lateral displacement (v) between the upper and lower halves of the specimen. Its value before the initiation of the kink band was quite small and was primarily due to slight distortions of the testing apparatus. During the dynamic load drop, v experiences a jump of 0.048 in (1.219 mm). This, of course, was the lateral displacement associated with the formation of the kink band (see inset in Fig. 3b). Immediately after the load jump, the specimen was unloaded and examined. An inclined kink band which started from the point of indentation and run across the width of the specimen had formed. The kink band had an average inclination, β, of 15.5° with a variation of approximately 14–18°, the higher values being close to the two edges of the specimen (V and K, 1997). The average width, w, of the band was 303 h ($h = 7$ μm) (measured in the direction of the rotated fibers). Inside the band, the fiber average rotation, $\bar{\phi}$, was 31°. In addition, a sliver of the plate was found to have split off the free edge opposite the indented side. Because of this splitting, the stress measured after the 'jump' is scaled according to the estimated new load-bearing area of the specimen which, in this case, was approximately 12% smaller than the original area.

After measurements of the kink band characteristics were taken, the sapphire plate and the steel plate with the window were inserted in the assembly, as shown in Fig. 2, and loading was resumed at the same displacement rate. During this phase of the experiment, in addition to the other measurements, digital photomicrographs of the kink band were taken as discussed in the previous section. The camera was synchronized with the data acquisition system which allowed us to subsequently identify the location of the micrographs on the σ–δ and σ–v responses in Fig. 3 (with ○).

During reloading, the initial part of the σ–δ response had a slope of approximately 7.3 msi (50 GPa), that is, approximately one half of the initial modulus of 15 msi (103 GPa). The stress stabilized at a plateau level of approximately 61 ksi (421 MPa) indicating that a steady-state deformation pattern had been achieved. This value of the plateau stress is defined as the propagation stress (σ_P) of the material. Both δ and v continued to increase under this applied stress. At an end shortening of 2.55%, we choose to terminate the test by unloading. The σ–δ as well as the σ–v responses were seen to exhibit significant nonlinearity during unloading.

Turning to the deformation inside the kink band, first we consider the sequence of digital pictures of the kink band taken during this test. Before reassembling the set-up, thin vertical lines were drawn on the region to be monitored at the upper and lower boundaries of the band. The lines served as an aid to visualizing the extent to which the band broadens. Thirteen configurations were recorded corresponding to the points identified with empty bullets on the responses in Fig. 3. A subset of six of the configurations from the loading part of the experiment are shown in Fig. 4.

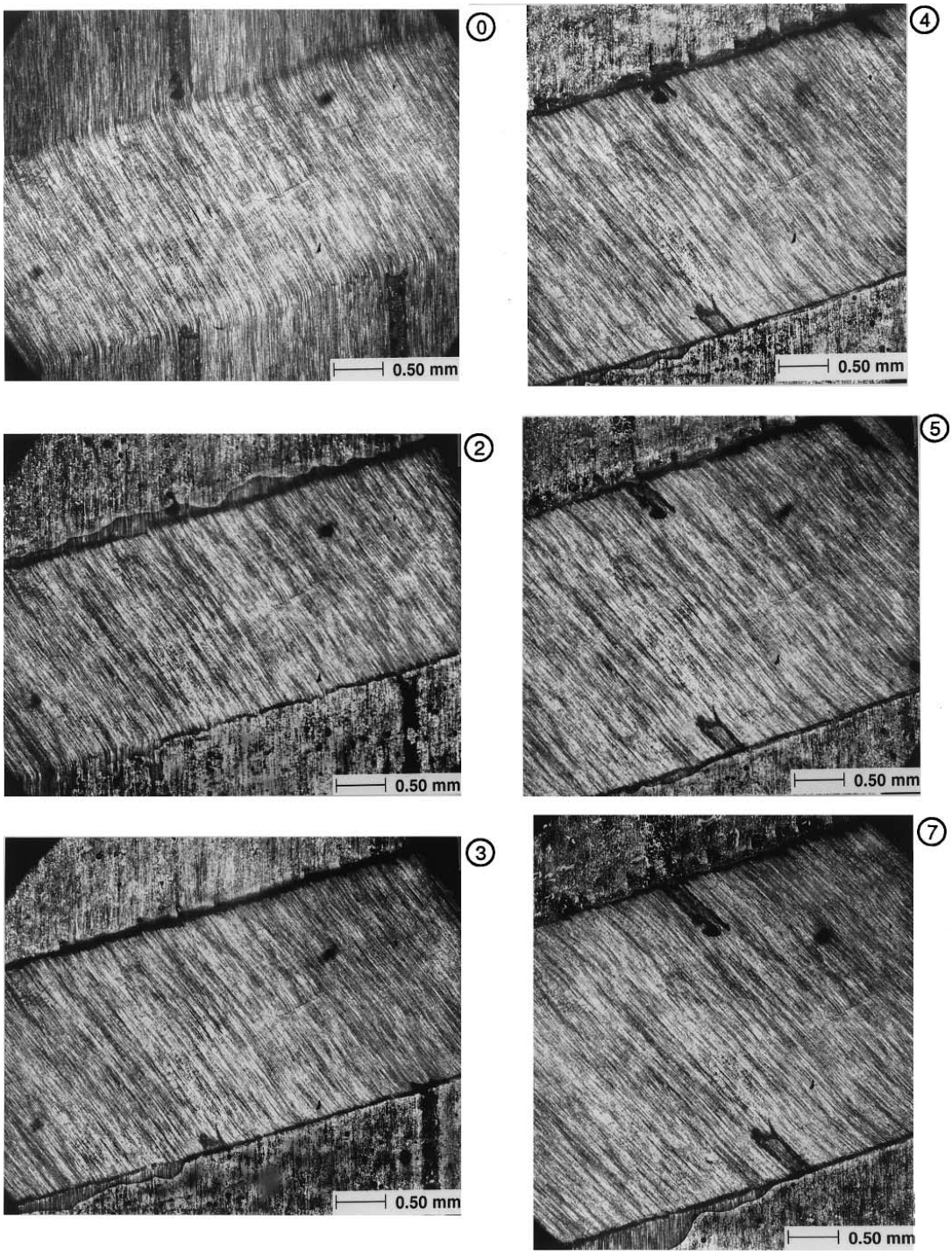

Fig. 4. Set of digital micrographs showing the evolution of a kink band during broadening (correspond to points identified on the responses in Fig. 3).

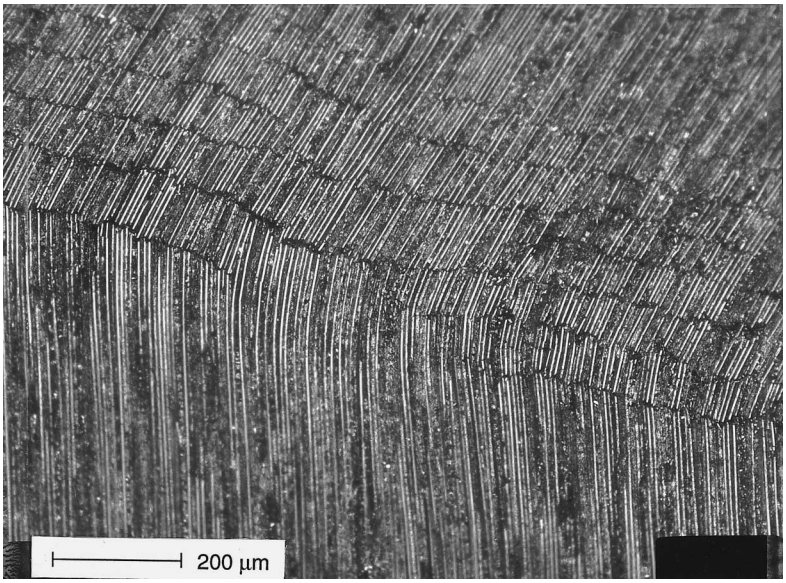

Fig. 7. Micrograph of features at the edge of a kink band.

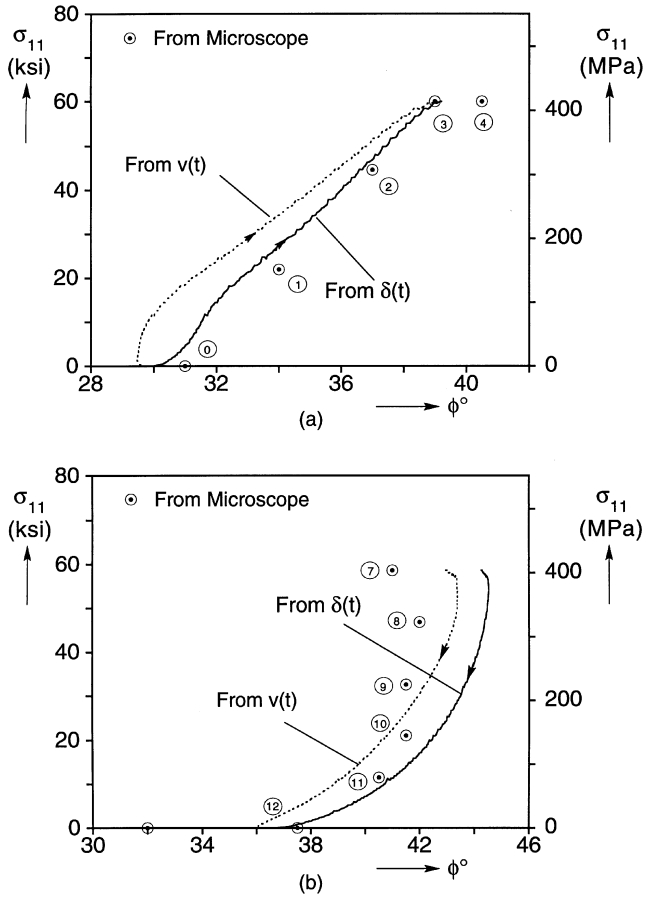

Fig. 5. Axial stress-fiber rotation response during (a) the loading and (b) the unloading of the specimen shown in Fig. 3.

Measurements of the band inclination β, its width w and of the fiber rotation ϕ were taken directly from the 2–3 mm section of the kink band shown in these micrographs.

The discrete values of ϕ during the loading portion of the test (configurations ⓪ to ④) were plotted as a function of the applied stress in Fig. 5a and for the unloading portion of the test (configurations ⑦ to ⑫) in Fig. 5b (identified by ⊙). The measured values of w from all thirteen configurations were plotted as a function of the stress in Fig. 6. The values of β, ϕ, and w at zero load (⓪) were respectively 15°, 31°, and 310 h. The vertical construction lines were seen to stop at the upper and lower boundaries of the band. As the band was loaded, its edges became more distinct (see ②), and fibers inside it rotated (34° at ①, 37° at ②). However, the band width remained the same (Fig. 6). By configuration ③, the stress level had risen to σ_P and band propagation had commenced. This was evident from the first crossing of the construction lines inside the band which now had a width of 356 h, while ϕ had increased to 39°. From configuration ④ to ⑦, ϕ remained essentially unchanged (fluctuates between 40° and 41°) while the band width

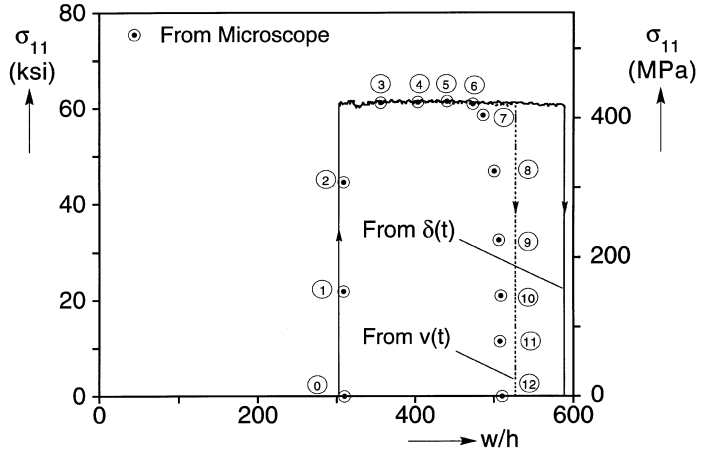

Fig. 6. Axial stress-kink band width response during the propagation phase of the test shown in Fig. 3.

steadily grows as seen in Figs. 4 and 6. At ⑦, just before unloading commences, the width reaches 486 h. By this time, the local value of β has also increased slightly to 17°.

During the unloading, the band width remained constant (see Fig. 6). Fiber rotation remained relatively unchanged until configuration ⑩ and subsequently decreased. By the time the specimen was fully unloaded and was out of the device ϕ returned to 32°.

The fiber rotation angle and the kink band width could also be estimated from the displacement histories $\delta(t)$ and $v(t)$ recorded by the two local transducers used in our set-up. Simple geometric considerations yielded the following relationships between the kink band variables

$$\delta = w(1-\cos\phi) + \frac{\sigma_{11}}{E'_{11}}L \tag{1}$$

and

$$v = w\sin\phi \tag{2}$$

where σ_{11} is the applied compressive stress, E'_{11} is the measured initial modulus of the intact composite, and L is the height of the specimen (we neglected the increased compliance of the kinked material).

In principle, (1) and (2) could be solved simultaneously for the two unknown quantities ϕ and w. However, because of their approximate nature we limited their use to estimating ϕ for the parts of the test when w does not change (i.e., for $\sigma_{11} < \sigma_P$) and used the values of w measured directly from the digital micrographs. Values of ϕ estimated from $\delta(t)$ using (1) and from $v(t)$ using (2) are included in the two plots in Fig. 5. During the loading phase of the test (Fig. 5a), agreement between these two continuous σ_{11}–ϕ responses and the discrete measurement was quite good. The value of ϕ is seen to increase from about 30° at zero stress to about 40° at the propagation stress. The angle increases nearly linearly with the applied stress, except for the initial parts of the two responses. We suspected that these initial transients were due to friction in the slider device. The variation of ϕ for the unloading portion of the response is shown in Fig. 5b. The two continuous

responses agree qualitatively with the discrete data, but some quantitative difference is present, especially for the results from $\delta(t)$.

We also used eqns (1) and (2) to trace the evolution of w during this test as follows. During the loading and unloading, w was assumed to have the constant values measured directly from the micrographs. During the band broadening phase of the test, the angle ϕ was assumed to remain constant at 41°. The results of this exercise can be seen in Fig. 6. Overall, the three sets of results are in reasonable agreement. During unloading, some quantitative difference between the predictions from $\delta(t)$ and those of the other two sets of measurements were observed once more.

The mechanism of kink band propagation was described in V and K (1997) as progressive addition of narrow zones of broken fibers at the edges of the kink band. Additional support for this sequence of events can be seen in Fig. 7. The kink band shown is in an unloaded state and has the following average parameters: $\bar{\beta} = 15.5^\circ$, $\bar{\phi} = 32^\circ$ and $\bar{w} = 400\ h$. Fibers inside the band (top of micrograph) are rotated a uniform amount, while those outside the band (bottom of micrograph) are straight and vertical. As the loading progresses, the straight fibers at the edge of the band bend as seen, for example, in the middle of this micrograph. Continued bending causes the fibers to break off as seen in the lower right of the micrograph. Such segments continue to rotate until they align themselves with the rest of the band. These segments have lengths in the range of 5 h to 13 h.

In the band micrograph sequence in Fig. 4, the kink band is seen to always have distinct edges formed mainly by broken fibers. Close examination of video recordings of the activity at the edges of the bands suggests that the boundary of the kink band is not perfectly straight and that it moves in a somewhat irregular manner. In some parts of the boundary, the bend–break–rotate sequence proceeds rapidly while in other parts no significant changes occur. Then, the inactive regions go through the process while the previously active regions remain temporarily inactive. Also, the propagation of the kink band is generally not equally balanced between the top and bottom of the band. It appears that at any given time one side is more active than the other.

A series of similar experiments were conducted at the baseline displacement rate of 0.008 in/min (0.2 mm/min) in order to test the repeatability of the results. Results from eight such experiments are summarized in Table 2. Failure initiated at stress levels between 103 and 116 ksi (710–800 MPa). The propagation stress varied between 61 and 77 ksi (421–531 MPa) and had an average value of 69.6 ksi (480 MPa) (the value of 68.8 ksi (474 MPa) reported in V and K (1997) was

Table 2
Kink band initiation stresses, characteristic angles, and propagation stresses from eight experiments ($\dot{\delta}/h = 5 \times 10^{-1}\ \mathrm{s}^{-1}$)

	σ_I ksi (MPa)	$\bar{\beta}^\circ$	$\bar{\phi}^\circ_U$	$\bar{\phi}^\circ_P$	σ_P ksi (MPa)
Average	109.6 (756)	15.5	30.5	40.5	69.6 (480)
Range	103–116 (710–800)	13–17	27–33	40–42	61–77 (421–531)
No. of Specimens	8	8	8	4	8

based on only four experiments). As pointed out earlier, during the initial dynamic initiation of the kink bands some splitting of the specimens took place. At least part of the variation in σ_P is due to the difficulty of accurately determining the load bearing cross sectional area of the specimen and/or deciding exactly when the split section stopped carrying load. The kink bands had an average inclination of 15.5°.

The kink band variables were monitored directly during the propagation phase in four experiments. The rotation of the fibers at the propagation stress, ϕ_P, ranged between 40° and 42°. By contrast, the fiber rotation in the unloaded state (ϕ_U) ranged between 27° and 33° with the average value from 8 experiments being 30.5°.

3.2. Effect of rate on the propagation stress

The process through which intact material is added to the kink band involves combined shear and transverse loads. These are the modes of loading in which the matrix nonlinearity (see Appendix in Kyriakides et al. 1995) and any rate dependence will come into play. Indeed, rate dependence was observed in the experiments in V and K (1997) and in the present ones during pauses in loading and at the termination of the stress plateau. It is also important to realize that once the band is formed and is propagating axially, the local 'strain rate' in the narrow zone of material ($\sim 10\,h$ wide) where the bend-break-rotate sequence is occurring is quite significant even at relatively slow end displacement rates. The increase in strain rate from that experienced by the material during the initial homogeneous deformation phase of the experiment is of the order of $L/10\,h$ (~ 700 for our specimens). Since the rate dependence of the nonlinear behavior of this composite is well documented (e.g. Yoon and Sun, 1991), we felt that some effect of rate on the propagation stress was to be expected.

We first undertook the task of establishing the rate dependence of our composite. This was accomplished through a set of pure shear, transverse compression, and biaxial experiments involving combinations of these two all conducted for a range of strain rates. The bulk of these results and those of associated modelling efforts will be reported independently. However, an impression on the extent of the rate dependence of the composite can be developed from the set of pure shear results shown in Fig. 8. The experiments involve pure shear loading of a long strip of the composite conducted in a custom testing facility at constant strain rates. Shear responses at rates spanning five decades in the range of interest to this application ($10^{-5} \leqslant \dot{\gamma} \leqslant 10^{-1}\ s^{-1}$) are shown. The increase in the shear stress with strain rate is quite obvious.

Having established that rate plays a significant role in the nonlinear behavior of the material, several additional experiments were conducted to measure directly the effect of rate on the propagation stress. As we have already shown, the measurements of σ_P exhibit some scatter. In order to separate the influence of rate from this scatter, the experiments were conducted as follows: a kink band was initiated in a specimen in the manner already discussed; the kink band was then propagated at a preselected displacement rate ($\dot{\delta}$) until a well defined propagation stress plateau was established; the displacement rate was then changed and the experiment was continued. Following a brief transient, the stress stabilized at a new stress plateau, either higher or lower than the first one depending on whether $\dot{\delta}$ was increased or decreased. This process enabled us to establish the difference between the two stress plateaus from the same specimen. A change of two

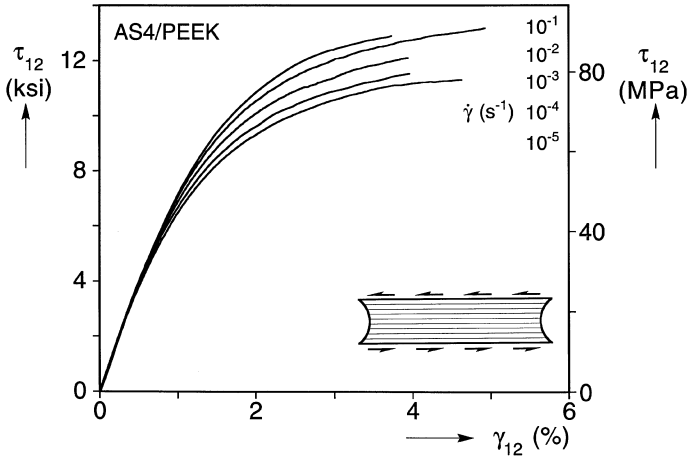

Fig. 8. Shear stress-strain responses of the composite at various strain rates.

orders of magnitude in loading rate was found to result in a clearly distinguishable change in the propagation stress.

Axial stress-end displacement responses from two such experiments are shown in Fig. 9. Other problem variables are given in Table 3. The rate of loading is quoted in normalized form as $\dot{\delta}/h$. In addition, in Fig. 9 the stress in each experiment is normalized by the lower of the two propagation stresses. In the experiment corresponding to Fig. 9a, the band is first broadened at a rate of $\dot{\delta}/h = 6 \times 10^{0}\ s^{-1}$. The propagation stress (σ_{P1}) is 70.8 ksi (488 MPa). At an overall strain of 1.7% the rate was reduced by two decades to $\dot{\delta}/h = 6 \times 10^{-2}\ s^{-1}$. Following a brief transient, the stress settles to a lower plateau level (σ_{P2}) of 63.8 ksi (440 MPa). In other words $\sigma_{P1}/\sigma_{P2} = 1.11$.

Results from the second experiment are shown in Fig. 9b. In this case, the slower rate was applied first and the fast rate second. After initiation, the kink band was propagated at a rate of $6 \times 10^{-2}\ s^{-1}$. The propagation stress (σ_{P1}) was found to be 68.6 ks (473 MPa). When the rate was switched to $6 \times 10^{0}\ s^{-1}$, the stress stabilized at a new plateau level (σ_{P2}) of 75.7 (522 MPa). The extent of the transient is seen in the figure to be of the same magnitude as the one in the previous experiment. Thus, once more, the two decades switch in rate changed the propagation stress by 10% ($\sigma_{P1}/\sigma_{P2} = 1.10$). Additional test results conducted in approximately the same displacement rate regime ($\dot{\delta}/h$ one decade higher and one lower) were consistent with this 10% change in σ_P per two decades change in $\dot{\delta}/h$. Due to the size of the specimens used, these experiments had to be conducted in a 225 kip (1 MN) capacity universal testing machine. Since the range of displacement rates that can be applied in a machine of this size is limited, a broader rate sensitivity study of σ_P was not possible.

4. Conclusions

Additional experiments have been presented showing that under compression aligned fiber composites can exhibit significant post-failure strength and ductility. The onset of failure is a dynamic event and results in kinking of fibers in well defined inclined bands. Under displacement

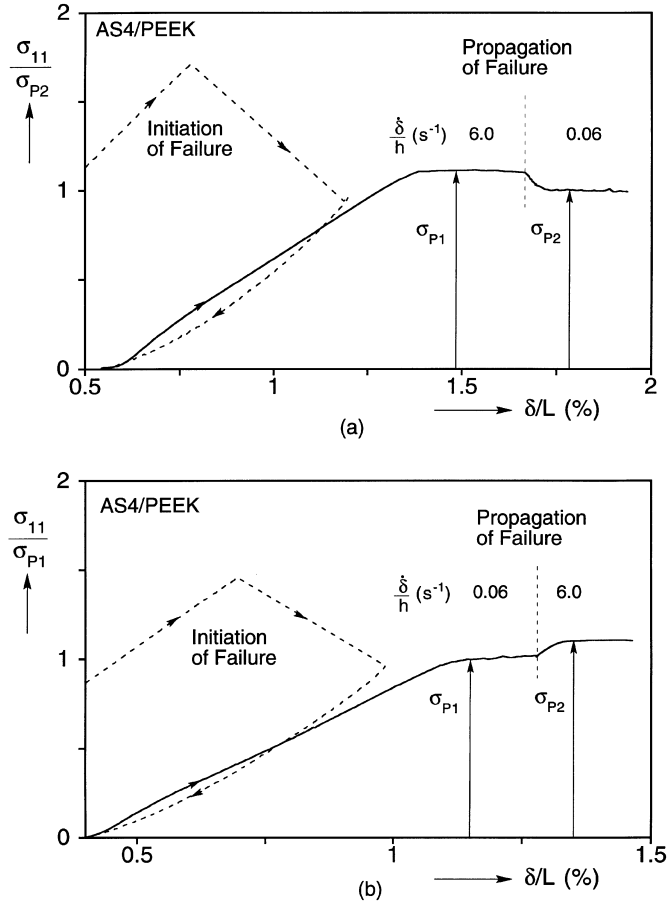

Fig. 9. Axial stress-end shortening responses for tests in which the loading rate was (a) decreased and (b) increased by two decades during steady-state propagation.

Table 3
Effect of end displacement rate on measured propagation stress

Spec. No.	σ_I ksi (MPa)	$\bar{\beta}^\circ$	ϕ_U°	$\dot{\delta}_1/h$ s^{-1}	σ_{P1} ksi (MPa)	$\dot{\delta}_2/h$ s^{-1}	σ_{P2} ksi (MPa)
I	109.1 (752.4)	15	30	6×10^{0}	70.8 (488)	6×10^{-2}	63.8 (440)
II	99.8 (688.3)	15	30	6×10^{-2}	68.6 (473)	6×10^{0}	75.7 (522)

controlled quasi-static loading, such bands have been shown to propagate axially (broaden) at a well defined stress level, called the *propagation stress* of the composite. As pointed out in V and K (1997), the measurement of this stress must be conducted under specific experimental conditions for it to be characteristic of the bulk material. The *propagation* stress of our AS4/PEEK composite was found to be of the order of 70 ksi (483 MPa) which compares with the compressive strength of the material of 175 ksi (1207 MPa).

The kink band inclination angle of AS4/PEEK is typically 15° which is set during the dynamic initiation of the band. The fibers inside such bands were found to be rotated at approximately 30° in unloaded states, but under load this rotation was shown, by direct measurements, to increase so that at the propagation stress it reached 40°. Thus, the assumption commonly made until now that $\phi = 2\beta$ is not correct in the presence of a load.

Broadening of the band is by successive addition of narrow zones of fibers from the intact material adjacent to it. Such zones, which typically were 10 fiber diameters wide, bend, break off the intact composite, and then rotate and align themselves with the rotated kink band material. Because of the rather small width of the deforming zone, the rate of deformation there is quite significant, even at relatively slow end displacement rates. At the displacement rates of our tests, the band was observed to propagate primarily on one front at a time.

The shear response of AS4/PEEK has been measured at strain rates spanning five decades and found to exhibit significant rate sensitivity. Since the main deformation mechanism during kink band propagation is shearing, the propagation stress is also rate sensitive. It has been shown that a two decade change in end displacement rate results in approximately a 10% change of σ_P.

Acknowledgements

The financial support of the Office of Naval Research under contract N00014-97-1-0515 is acknowledged with thanks as is the cooperation of Dr. Y.D.S. Ravjapakse in his capacity as one program director. The work of TJV was also supported by the Fannie and John Hertz Foundation and the W.M. Keck Foundation.

References

Budiansky, B., Fleck, N.A., Amazigo, J.C., 1997. On compressive kink-band propagation. Journal of the Mechanics & Physics of Solids (to appear).

Chaplin, C.R., 1977. Compressive fracture in unidirectional glass-reinforced plastics. Journal of Materials Science 12, 347–352.

Evans, A.G., Adler, W.F., 1978. Kinking as a mode of structural degradation in carbon fiber composites. Acta Metallurgica 26, 725–738.

Fleck, N.A., Budiansky, B., 1991. Compressive failure of fibre composites due to microbuckling. Proc. IUTAM Symposium on Inelastic Deformation of Composite Materials, Ed. G.J. Dvorak, pp. 235–273, Springer-Verlag, NY.

Fleck, N.A., Sivashankar, S., Sutcliff, M.P.F., 1997. Compression failure of composites due to microbuckle growth. European Journal of Mechanics: A/Solids 16 (Suppl. 5), 65–82.

Kyriakides, S.K., Arseculeratne, R., Perry, E.J., Liechti, K.M., 1995. On the compressive failure of fiber reinforced composites. International Journal of Solids & Structures 32, 689–738.

Kyriakides, S.K., Ruff, A.E., 1997. Aspects of the failure and postfailure of fiber composites in compression. Journal of Composite Materials 31, 1999–2037.

Moran, P.M., Liu, X.H., Shih, C.F., 1995. Kink band formation and band broadening in fiber composites under compressive loading. Acta Metallurgica et Materialia 43, 2943–2958.

Moran, P.M., Shih, C.F., 1997. Kink band propagation and band broadening in ductile matrix fiber composites: experiments and analysis. Int'l Journal of Solids & Structures (to appear).

Paterson, M.S., Weiss, L.E., 1966. Experimental deformation and folding in phyllite. Geological Society of America Bulletin 77, 343–374.

Sivashanker, S., Fleck, N.A., Sutcliffe, M.P.F., 1995. Microbuckle propagation in a unidirectional carbon fiber-epoxy matrix composite. Acta Materialia 44, 2581–2590, 1996.

Steif, P.S., 1990. A model for kinking in fiber composites-II. Kink band formation. International Journal of Solids & Structures 26, 563–569.

Vogler, T.J., Kyriakides, S., 1997 Initiation and axial propagation of kink bands in fiber composites. Acta Materialia 45, 2443–2454.

Weaver, C.W., Williams, J.G., 1975. Deformation of a carbon-epoxy composite under hydrostatic pressure. Journal of Materials Science 10, 1323–1333.

Yoon, K.J., Sun, C.T., 1991. Characterization of elastic-viscoplastic properties of an AS4/PEEK thermoplastic composite. Journal of Composite Materials 25, 1277–1296.